$Bi_2Sr_2CaCu_2O_{8+\delta}$ intrinsic Josephson junctions in a magnetic field

A. Yurgens,* D. Winkler, and T. Claeson
Department of Microelectronics and Nanoscience, Chalmers University of Technology, S-41296, Göteborg, Sweden

G. Yang, I. F. G. Parker, and C. E. Gough
Superconductivity Research Group, University of Birmingham, Birmingham B15 2TT, United Kingdom
(Received 1 June 1998)

The normal and superconducting state *c*-axis transport properties of $Bi_2Sr_2CaCu_2O_8$ single crystals have been measured as a function of doping and magnetic fields parallel and perpendicular to the CuO_2 planes, using mesa structures containing a small number of atomic unit-cell layers. For low current bias, the peak in the magnetic-field-dependent *c*-axis resistance is observed to scale approximately inversely with the zero-field critical current. The critical current I_c is strongly dependent on temperature and field $B_\perp$ perpendicular to the CuO_2 planes. This provides information on the magnetic phase diagram and the correlation of flux pancakes across adjacent pairs of superconducting CuO_2 planes. Over an appreciable region of the phase diagram the critical current $I_c(B_\perp)$ varies $\sim 1/B_\perp^\mu$, with $\mu \approx 0.8$ to 0.9. In a parallel field, $I_c(B_\parallel)$ varies as $\exp[-(B_\parallel/B_0)]$, with $B_0 \sim 2$ T, consistent with a model involving pinned Josephson vortices. [S0163-1829(99)07909-6]

INTRODUCTION

Measurements of the *c*-axis, out-of-plane, electrical transport properties are of great importance in probing the vortex system properties of highly anisotropic layered high-T_c (HTc) compounds, such as $Bi_2Sr_2CaCu_2O_8$ (2212-BSCCO). In such superconductors, vortex lines are formed from vortex ''pancakes'' with circulating currents confined to the CuO_2 planes. The pancakes interact with each other magnetically and via interlayer Josephson coupling.[1–4] In an ideal layered superconductor at low temperatures, these interactions encourage pancakes to align perpendicular to the planes. However, when the interlayer interactions are weak, thermal fluctuations and local pinning centers cause misalignment. This leads to a loss in phase coherence between adjacent pairs of superconducting planes and hence a reduction in the critical current.

The concept of flux pancakes implies the use of the Lawrence-Doniach model to describe the layered high-T_c compounds.[5] The observation of both dc and ac Josephson tunneling across individual planes in the layered HTc compounds have confirmed the validity of such a model for highly anisotropic HTc superconductors.[6,7]

The majority of previous measurements of the *c*-axis electrical characteristics have been made using single crystals, in which the Josephson nature of the interlayer coupling has simply been assumed, without any direct justification. For example, authors often cite the hysteretic current-voltage (*I-V*) characteristics as evidence for Josephson tunneling.[8,9] Although consistent with such an interpretation, the published characteristics have usually been made across a large number of junctions, often with a wide range of critical currents. The *I-V* characteristics of bulk crystals can be severely affected by Joule heating due to their relatively large thickness.[8] In addition, mm-sized single crystals are unlikely to be free of structural defects. The *c*-axis conduction in such crystals may then involve a mixed array of parallel and series intrinsic Josephson junctions (IJJ's). The commonly used technique of stabilizing silver-paint contacts by annealing at an elevated temperature (typically in the range 300–600 °C) inevitably leads to the diffusion of silver in the *c* direction and along any micro-cracks near the surface. The characteristics of the surface-damaged regions can therefore obscure the intrinsic interlayer characteristics of the bulk crystal. Moreover, any high-temperature processing will result in the diffusion of oxygen in or out of the sample, so that the level of doping is undetermined.

We overcome such problems by making measurements on small area (10×20 to 20×30 μm^2) mesa structures, typically a few unit cells in height, lithographically patterned on the surface of freshly cleaved 2212-BSCCO single crystals,[10] using standard photolithography with chemical and/or Ar-ion beam etching. The latter was performed at liquid-nitrogen temperatures to avoid excessive sample heating. Subsequent lithography and patterning were performed at relatively low temperatures (<140 °C), to minimize any problems of silver or oxygen diffusion in the uppermost layers of the structure.

In this paper, we report measurements of the field-dependent *c*-axis tunneling characteristics across the intrinsic interplanar Josephson junctions in epitaxial 2212-BSCCO mesa structures. Such measurements probe the interplanar pancake correlations on an atomic interlayer length scale, complementing measurements of vortex correlations on the much longer length scales involved in low-angle neutron-diffraction,[11] μSR,[12] magnetic,[13,14] and bulk transport[15,16] measurements. If we assume a sinusoidal phase relation, the critical current can also be related to the microwave plasma resonance.[17,18] The *c*-axis transport measurements were made over a wide temperature range, in fields up to 6 T, perpendicular and parallel to the planes. Measurements were made on a number of mesa structures on the surface of two crystals with different oxygen content and hence anisotropy factors, $\gamma=(\lambda_c/\lambda_{ab})^{1/2}$, where the subscripts refer to current flow along the *c*-axis and *ab*-plane directions. The mesa volume under study is about six orders of magnitude smaller than that of the bulk crystals typically

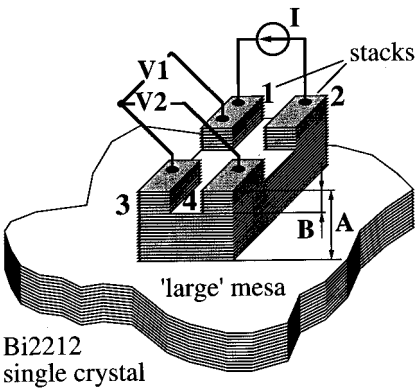

FIG. 1. Schematic view of the configuration of potential and current leads used to study a particular stack (top left). Using the same current connections, the voltage $V1$ is proportional to ρ_c, while the voltage $V2$ monitors the in-plane voltage, approximately proportional to $(\rho_c\rho_{ab})^{1/2}$, though absolute measurements cannot be made because of the undefined geometry (Ref. 24).

used in previous studies. This largely eliminates problems from heating and crystalline defects.

Essentially identical and reproducible, multibranched, *I-V* characteristics were observed for all mesas on the same crystal. The branches correspond to the individual Josephson junctions in the mesa stack switching in turn to the resistive state. The *c*-axis critical current $I_c(T,B)$, resistance $R_c(T,B)$, and detailed form of the *I-V* characteristics were measured as a function of temperature and magnetic field in both the perpendicular and parallel configurations. The measurements have been interpreted in terms of the alignment of pancake vortices across adjacent pairs of CuO_2 planes, providing information on the rich magnetic phase diagram of 2212-BSCCO.[19]

EXPERIMENT

The single crystals were grown using a large temperature gradient growth technique.[20] The oxygen content and hence degree of anisotropy was varied by annealing the parent crystals in argon or oxygen prior to fabrication of the mesa structures. The magnetic properties of crystals from the same growth and processing batch were characterized by superconducting quantum interference device (SQUID) magnetometry giving an independent measure of T_c and the γ-dependent, three-dimensional–two-dimensional, (3D-2D) vortex dissociation field, identified as the onset of the arrowhead anomaly.[21–23]

Four mesa structures with up to four contacts, separated from each other by a slot ion beam milled into the body of the mesa, were lithographically patterned on the cleaved surface of the single crystals.[10] Using separate voltage and current contacts on three mesas, we were able to make 4-point measurements of the *c*-axis *I-V* characteristics across a selected mesa $V1$ and I in Fig. 1. Measurements involving a fourth mesa enabled us to monitor the voltage $V2$ associated with current flow parallel to the *ab* plane. Absolute measurements in this configuration were not possible because of the undefined spatial current distribution.

In the superconducting state $V2$ was always near zero, as expected for an epitaxially layered superconductor, where for small current bias the only voltage drop occurs across the measured stack. In the normal state, the in-plane voltages $V2$ were typically $<5\%$ of the *c*-axis voltage $V1$ across the selected mesa. Contributions to $V2$ arising from nonuniform current flow in the normal state were therefore assumed to be very small. This was also consistent with the very different field and temperature dependence of the resistance $R_c = V1/I$ and $R_{ab} = V2/I$, measured using a small current bias ($\sim$1–2 A cm^{-2}) at $\sim$37 to 47 Hz.

In the superconducting state the multibranched *I-V* characteristics were recorded digitally from multiple traces generated using a 43 Hz triangular-waveform bias current, which was 100% amplitude modulated at $\sim$11 Hz, to provide sweeps of varied amplitude. The current and voltage were monitored with low-noise instrumentation amplifiers and were digitized at an uncorrelated frequency. This enabled us to record a large number of the individual branches.

The sample was cooled by helium exchange gas in a continuous-flow cryostat, enabling measurements to be made from $\sim$6 K to room temperature. The *ab* plane of the sample was oriented parallel or perpendicular to the externally applied magnetic field to an estimated accuracy of $\sim$0.5°.

We present measurements for mesas $\sim 20\times30\times0.02$ μm^3 on the surface of an oxygen-annealed (slightly overdoped) and an argon-annealed (slightly underdoped) crystal.

NORMAL-STATE PROPERTIES AND MAGNETORESISTANCE IN A PERPENDICULAR MAGNETIC FIELD

Figure 2 shows the temperature dependence of R_c [Fig. 2(a)] and R_{ab} [Fig. 2(b)] for the oxygen-annealed sample measured at several fields parallel to the *c* axis. $R_c(T)$ develops a pronounced peak below the zero-field transition temperature $T_c(0)$, whereas $R_{ab}(T)$ falls monotonically towards zero, but with a shoulder resulting from the increased anisotropy, since $R_{ab}\sim(\rho_c\rho_{ab})^{1/2}$ for currents flowing parallel to the surface.[24] For comparison, we have also included a single 6 T measurement for the argon-annealed sample. This exhibits a resistance peak almost twice as large as for the oxygen-annealed sample, whereas the zero-field critical current at low temperatures is approximately halved (Fig. 3). This suggests an inverse relationship between the magnitude of the resistive peak and the critical current density.

For the argon-annealed sample, the peak in R_c is almost nine times the normal state resistance at $T=160$ K. This is one of the highest ratios ever reported.[25–30] The difference between our argon- and oxygen-annealed samples can almost certainly be attributed to differences in oxygen content and hence anisotropy factor γ. The absolute magnitudes of critical currents and resistivities are qualitatively similar to those reported by previous authors.[9,26–29] However, there are significant differences. For example, in Ref. 28 both oxygen- and argon-annealed crystals exhibited very similar peaks in R_c. Furthermore, for the quoted value of critical current for the oxygen-annealed crystal in Ref. 9, the reported peak in R_c is about a factor of 3 smaller than expected from our measurements, assuming the same inverse relationship between peak height and critical current. These differences may be related to the high-temperature annealing (500–

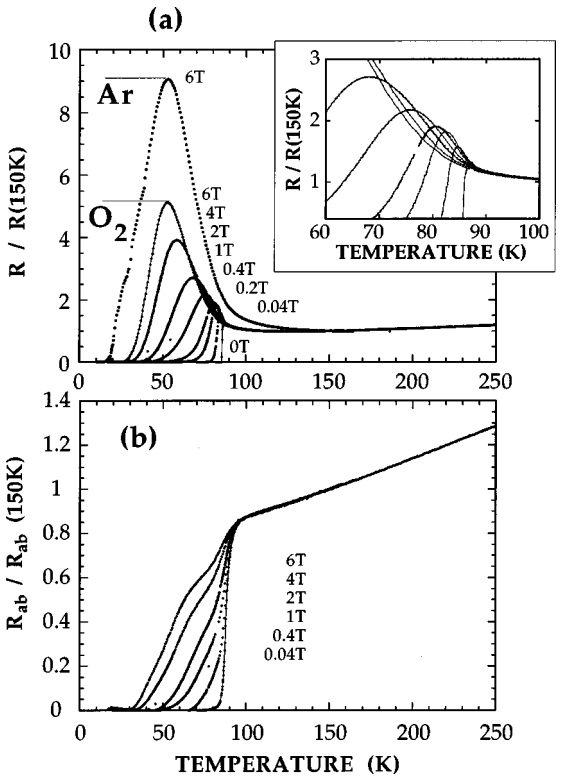

FIG. 2. Temperature dependence of (a) the out-of-plane and (b) in-plane voltages for the oxygen-annealed sample in a perpendicular magnetic field. Only one curve is shown for the argon-annealed sample. The inset shows an enlarged part of the dependence close to T_c.

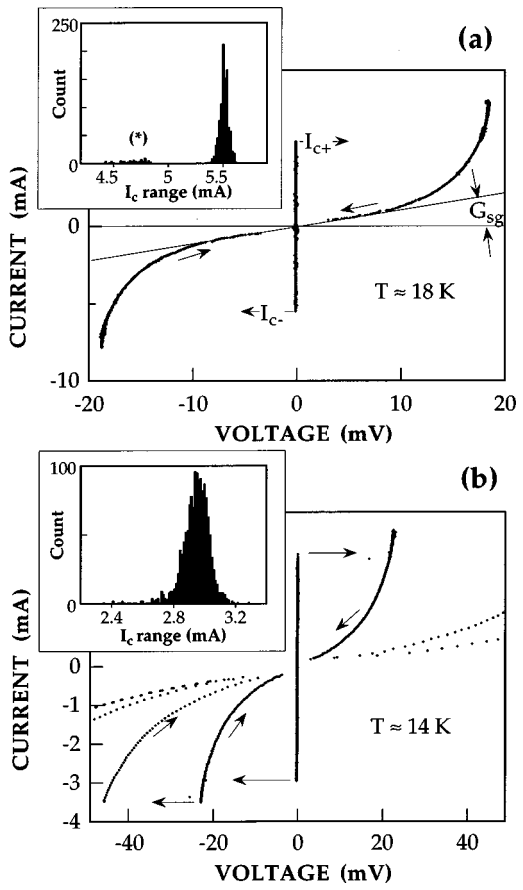

FIG. 3. Typical *I-V* characteristics of nearly identical stacks of 1D array of intrinsic Josephson junctions in zero magnetic field at low temperatures and voltages. The insets show the critical current distribution functions $P(I_c)$ obtained from about 1000 measurements of the critical current I_c. (a) The first of 14 resistive branches for the oxygen-annealed sample. (b) The first two of 15 resistive branches for the argon-annealed sample. The arrows indicate the directions of multiple bias current cycles in tracing out the branches shown.

600 °C) used to stabilize the silver electrical contacts, which may result in partial shorting by silver diffusing into the structure or penetrating along microcracks.[9]

The temperature dependence of R_c in a perpendicular magnetic field was reported by Briceno, Crommie, and Zettl.[26] Below T_c in zero field, the temperature dependence was explained by phase slippage of the superconducting order parameter, though no explanation was provided for the higher-temperature ''semiconducting'' temperature dependence above the peak.[26] A number of authors have discussed the origin of the peak invoking both coherent and incoherent *c*-axis transport models (see Ref. 31 and references therein).

Ioffe *et al.* have shown that superconducting fluctuations can decrease the one-electron density-of-states (DOS) resulting in an increase in *c*-axis resistance.[32] Because the temperature variation of this contribution is less singular than the Aslamasov-Larkin contribution, it can dominate over an appreciable temperature range, giving rise to the peak in resistivity. Dorin *et al.* have considered the influence of perpendicular fields on the fluctuation contributions in this model.[33]

Gray and Kim proposed a rather similar model, treating the layered superconductor as a series array of Josephson junctions.[34] In this model also, the absence of phase coherence of the superconducting fluctuations across adjacent superconducting CuO_2 bilayers suppresses the *c*-axis pairing conductance above T_c. In a magnetic field, competition between the quasiparticle and pairing conductances across the junctions again accounts for the observed peak in *c*-axis resistance.

Although fluctuations may well contribute to the observed field and temperature dependence of the *c*-axis resistance, for our argon-annealed 2212-BSCCO crystal we have to account for a ninefold increase in resistance in large magnetic fields and a tenfold increase for some samples in zero field.[10,30] This is rather large to be explained by fluctuations alone, which are usually considered as a small perturbation to the tunneling.[32,33,35]

SUPERCONDUCTING STATE, ZERO-FIELD *I-V* CHARACTERISTICS

In the superconducting state the characteristics become highly hysteretic and multibranched,[6,7] as expected for a linear array of superconductor-insulator-superconductor (SIS) Josephson junctions with a large interlayer capacitance. Figures 3(a) and 3(b) include typical, low-temperature *I-V* characteristics of the first hysteretic branch for mesas patterned on our argon- and oxygen-annealed crystals, each mesa including a stack of about 14 intrinsic junctions. The arrows indicate the direction of the bias current sweep during the measurements.

For both samples, the dynamic conductance *dI/dV* on the

resistive branches becomes almost infinite before jumping to the next branch (see Fig. 3). The change in voltage V_g across layers at this transition can be used to define a characteristic energy, which in an ideal SIS junction would be twice the superconducting energy gap, $2\Delta/e$. Almost identical voltages are observed between all branches of the *I-V* characteristics. If we assume that the jumps are related to the superconducting energy gap, we obtain values for $\Delta(0)$ of $\sim$9 meV and $\sim$12 meV for the oxygen- and argon-annealed samples, respectively. These values are less than half the values expected from surface tunneling measurements on 2212-BSCCO crystals.[36,37] A smaller gap would be expected if the tunneling involved proximity coupling to intermediate metallic or semiconducting BiO layers. This would also account for the non-BCS temperature dependence of V_g reported in earlier measurements.[38] Nonequilibrium quasiparticle injection effects, and even local heating at large currents, may also decrease the measured gap.

For an intrinsic unshunted *s*-wave SIS junction, the conductance G_{sg} on the hysteretic-resistive, phase-slip, return path would become exponentially small at low temperatures, whereas the observed characteristics have a finite slope. This strongly suggests a finite density of quasiparticle states in the gap, consistent with *d*-wave rather than *s*-wave superconductivity.

Although the *I-V* characteristics on the return, phase-slip branches are highly reproducible, the current at which switching to the resistive branch takes place can vary appreciably from one measurement cycle to the next. In the highly hysteretic regime at low fields and temperatures, we define the critical current as the bias current at which the mesa switches to the first resistive branch. External or thermal noise can cause early transitions, yielding measured I_c values significantly less than the intrinsic critical current I_{c0}.[39] By automating our measurements, between 10^3 and 10^4 individual measurements could be accumulated giving a measured critical current distribution $P(I_c)$, as illustrated by the insets of Figs. 3(a) and 3(b). An operational critical current I_c can then be defined as the position of the peak of the distribution function. In plotting our measurements of the critical current in Fig. 4(c), the half-width of the distribution function has been indicated by error bars. The width is a strong function of both temperature and field. This reflects a real variation in critical currents from cycle to cycle rather than errors in the measurements themselves.

The critical current for the oxygen-annealed crystal is almost double that of the argon-annealed sample. We also observed a small number of early transitions well below the main peak for the oxygen-annealed sample, which could result from one of a number of metastable Josephson vortex configurations within the stack.[40]

At higher temperatures and fields, the characteristics become resistive at small currents because of thermally activated phase slip or flux flow; at sufficiently high temperatures the *I-V* characteristics become reversible. In these regimes operational critical currents can still be defined, either from the current required to give 0.1 μV across the stack or by extrapolating the *I-V* characteristics at finite voltages to zero voltage, as illustrated in Fig. 4(b). Above the temperature $T_{\rm irr}(B_\perp)$ at which a measurable resistance emerges (Fig. 2), the two definitions give very different values, illustrated by the open and closed circles in Fig. 4(c).

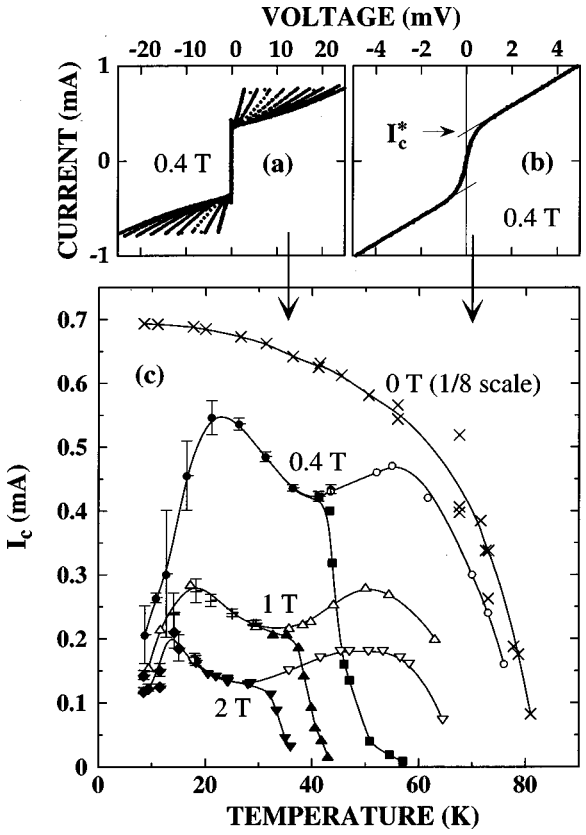

FIG. 4. (a) and (b): *I-V* characteristics of the oxygen-annealed sample in the perpendicular magnetic field of 0.4 T at $T=36$ K and $T=70$ K. (c) Temperature dependence of the *c*-axis critical current for perpendicular magnetic fields as indicated. Empty symbols represent the ''quasicritical'' current I_c^* defined in (b). Filled symbols correspond to the critical current I_c defined using a 0.1 μV voltage criterion or from the critical current distribution functions $P(I_c)$. The lines drawn through the experimental points are only intended as guides for the eye.

CRITICAL CURRENT IN A PERPENDICULAR MAGNETIC FIELD

Figure 4(c) shows $I_c(T,B_\perp)$ for the oxygen-annealed sample in magnetic fields of 0, 0.4, 1, and 2 T parallel to the *c* direction. All measurements were made on warming in a constant field, applied before first cooling from above T_c, to ensure as uniform a distribution of flux across the mesa as possible. Figures 4(a) and 4(b) show typical *I-V* characteristics at 0.4 T for the lower temperature, multibranched, hysteretic regime and for the higher-temperature, reversible regime, at the temperatures indicated by the arrows. Very similar results were obtained for mesas on the argon-annealed sample.

We first note the large decrease in critical current with applied field over the whole temperature range. At low temperatures, the decrease in critical current is particularly large—more than two orders of magnitude in a field of 6 T. On warming, the critical current in a finite field increases to a peak in the temperature range 15–25 K. At low temperatures the variation in critical current from cycle to cycle increases as the temperature decreases, as illustrated by the increased size of the error bars. This is contrary to what

would have been expected had thermal[41] or extrinsic noise been the dominant source of the variation. The fluctuations in critical current could be explained either by stochastic fluctuations in the pinned vortex state from one cycle to the next, or by different metastable configurations of Josephson vortices trapped between the planes.

Above the peak, the critical current decreases, but with no onset of any resistance at low current bias. However, at $T_{\rm irr}(B_\perp)$, which we identify as the irreversibility temperature, the characteristics become resistive at small voltages, as plotted in Fig. 2. This leads to a divergence of the two definitions of critical current as indicated in Fig. 4. However, apart from the onset of a finite resistance at small voltages, there is little change in the form of the *I-V* characteristics at $T_{\rm irr}(B_\perp)$. In particular, the ''excess current'' critical current $I_c^*(T,B_\perp)$ extrapolates smoothly to the values of the ''true'' $I_c(B_\perp)$ below $T_{\rm irr}(B_\perp)$. Interestingly, $I_c^*(T)$ goes through a weak minimum at $T_{\rm irr}(B_\perp)$ before rising again to a maximum at ~10–20 K above $T_{\rm irr}(B_\perp)$, and then falling towards zero at $T_c(0)$.

INTERPRETATION OF MEASUREMENTS

There has been considerable interest in the vortex states of 123-YBCO, 2212-BSCCO, and other high-T_c compounds. 2212-BSCCO is particularly interesting because of its extremely large anisotropy factor, making it one of the most two-dimensional of all HTc superconductors. A recent discussion of the magnetic phase diagram of 2212-BSCCO has been given by Goffman *et al.*,[42] which we can relate to the degree of *c*-axis correlation of pancakes inferred from our measurements.

On increasing the temperature in small fields ($\leqslant$50 mT), a first-order magnetic transition from an ordered 3D flux-line solid to a liquid state has been inferred from a number of measurements. The simultaneous onset of resistance is consistent with a vanishing shear modulus in the liquid state.[43]

However, on cooling in a field $\geqslant$50 mT, the low-temperature phase is believed to consist of a random array of pinned flux pancakes within the planes with little correlation within the CuO_2 planes or along the *c* axis. Nevertheless, μSR measurements at low temperatures (<20 K) in fields up to 0.15 T reveal an asymmetric distribution of local fields, with a high-field tail implying a residual degree of alignment in the *c* direction on a length scale $\sim\lambda_{ab}$.[44] In the transition region with fields ≈100 mT, increasing the temperature leads to an enhanced neutron-diffraction signal and a corresponding increase in the asymmetry of the μSR field distribution[44] indicating an increase in *c*-axis alignment on heating. This demonstrates the role of thermal activation in releasing flux lines from low-lying pinning sites (e.g., oxygen vacancies), enhancing their alignment along the *c* axis via electromagnetic or Josephson coupling.[1–4,45]

We can therefore account for the observed increase in critical current with increasing temperature in our measurements in terms of a progressive thermal depinning of flux pancakes and increased alignment along the *c* axis. The increased mobility of pancakes on warming may also account for the reduction in scatter of critical current values, as they can move more easily towards a nearly thermodynamic equilibrium configuration between measurements. Bulaevskii, Pokrovsky, and Maley have predicted an approximately linear increase in critical current with temperature in this regime, involving the thermal excitation of the low-lying normal modes of the pancake glass structure.[46]

On heating samples cooled in fields above ≈0.1 T, μSR experiments indicate a relatively sudden transition to a much more symmetric local-field distribution at around 20 K,[44] a temperature that is close to the peak in measured critical currents, where the scatter between measurements almost disappears. At about the same temperature there is also a pronounced change in magnetic creep rate.[47] These observations are consistent with a thermal depinning transition involving oxygen vacancies or other point defects, which inhibit the alignment of the pancakes between planes. As the temperature is further increased, thermal fluctuations reduce the degree of *c*-axis alignment and hence the critical current, as observed.

We note that the Kosterlitz-Thouless melting transition for a 2D vortex lattice is predicted to be ~20 K.[19] Interestingly, in measurements of the thermal conductivity κ of 2212-BSCCO in a magnetic field, a plateau in $\kappa(B)$ is observed below $T\sim$20 K.[48] However, the absence of any significant dissipation in the *c* direction in our measurements until well above this temperature suggests that we are still in a solid flux pancake phase above 20 K. The onset of resistance at $T_{\rm irr}(B_\perp)$ suggests that melting takes place at this temperature. This temperature coincides with the onset of hysteresis in magnetic measurements on the parent crystals, in good agreement with measurements on 2212-BSCCO by Fuchs *et al.*[43] (see Fig. 5). A phase change at this temperature is also confirmed from changes in local-field distribution deduced from μSR measurements on crystals from the same batch.[12]

In Fig. 5 we show the *B-T* phase diagram suggested by our measurements for fields perpendicular to the *ab* planes. The open symbols indicate the temperature T^* of the first peak in critical current, and the filled symbols the temperature $T_{\rm irr}$ marking the onset of resistivity along the *c* axis. Over a relatively wide range of fields, $T_{\rm irr}\propto\ln(1/B_\perp)$.

There appears to be a weak maximum in T^* at small fields, while at large fields it approaches the field-independent, 2D vortex lattice Kosterlitz-Thouless melting transition, $T_{\rm 2D}$.[19] This is consistent with the suppression of both Josephson and electromagnetic interlayer coupling at high fields, so that the system becomes increasingly two-dimensional.

T^* and $T_{\rm irr}$ define three regions of the *B-T* phase diagram. This involves two solid phases below $T_{\rm irr}$ where a zero-voltage, true *c*-axis supercurrent is observed, and a liquid phase above $T_{\rm irr}$ where the *c*-axis conduction is dissipative. T^* may mark the temperature at which both C_{44} and C_{66}, the elastic moduli of the vortex lattice, are predicted to vanish.[49] The phase between T^* and $T_{\rm irr}$ may represent a glassy state of vortices with long-range orientational order; whereas the transition to a more conventional liquid state does not occur until $T_{\rm irr}$.[49,50]

Above $T_{\rm irr}$, now identified as the liquid phase, earlier measurements by Busch *et al.*[24] imply that, over a wide range of fields, the in- and out-of-plane resistivities are characterized by the same thermal activation energy, suggesting a common origin for dissipation in both directions.[51]

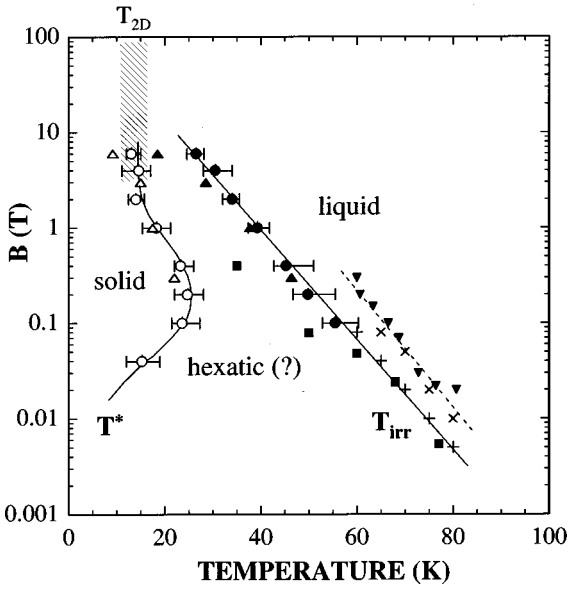

FIG. 5. *B-T* diagram of vortex phases for fields perpendicular to the *ab* planes suggested by our measurements. Empty symbols represent the field dependence of the temperature T^* at which the maximum of $I_c(B_\perp, T)$ dependence is observed [see Fig. 4(c)]. The solid symbols represent the irreversibility line $T_{\rm irr}(B_\perp)$ observed in different experiments: (■) μSR measurements;[12] (▼) melting line from Ref. 62, where multiterminal transport measurements in the flux-transformer configuration have been made; (×) and (+) irreversibility line inferred from the magnetization measurements of a 2212-BSCCO single crystal from the same batch as those used in the present study (upper triangles and circles, for the argon- and oxygen-annealed sample, respectively). Although the lines are only guides for the eye, the irreversibility temperature seems to obey a simple logarithmic dependence, $T_{\rm irr}(B_\perp) \propto -\ln(B_\perp)$, illustrated by the straight line in this semilogarithmic plot.

As remarked earlier, despite the onset of resistance at low voltages above $T_{\rm irr}$, it is still possible to define a critical current in terms of the ''excess current'' extrapolated to zero voltage, which varies smoothly through the melting transition regime, as illustrated in Fig. 4. The somewhat surprising existence of a critical current extending well into the liquid state is a consequence of the attractive Josephson or magnetic[4] coupling of pancakes between the planes. This results in a thermally averaged, partial alignment of the pancakes, as described by Koshelev.[52] This accounts for the persistence of the microwave Josephson plasma resonance at temperatures well above the irreversibility line.[17,18]

Although the rapid onset of a resistance at $T_{\rm irr}(B_\perp)$ suggests a first-order melting transition, as observed by Fuchs *et al.* at small fields,[43] the absence of any qualitative change in the *I-V* characteristics at the transition imply a second-order or thermally broadened phase transition at these higher fields. Our measurements suggest that there is little change in the correlation of flux pancakes in the *c* direction at the melting transition, with perhaps a significant fraction of pancakes remaining strongly pinned at this transition. This could also account for the slight increase of $I_c^*(T, B_\perp)$ on increasing temperature above $T_{\rm irr}(B_\perp)$ as such pancakes eventually become thermally unpinned, enabling them to move more freely and hence to optimize their thermally averaged alignment along the *c* direction.

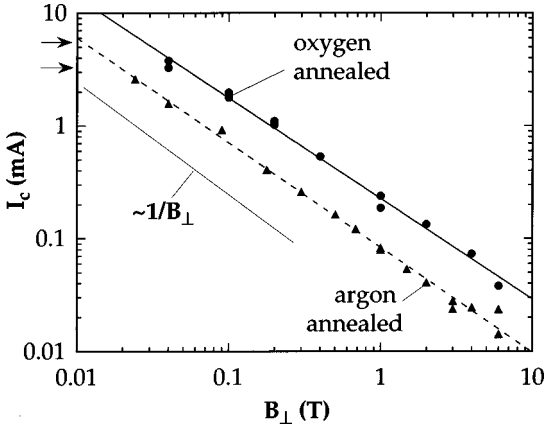

FIG. 6. $I_c(B_\perp)$ at $T=25$ K for the two samples with different oxygen content. The dependence $I_c \propto B_\perp^{-1}$ is shown for comparison.

In the low-temperature limit, Bulaevskii, Pokrovsky, and Maley[46] have predicted a power-law field dependence for the critical current with $I_c(0, B_\perp) \sim 1/B_\perp^\mu$, where $\mu=1$ for random disorder across the planes and less than unity for increased *c*-axis alignment. Koshelev predicts a similar field dependence for the Josephson coupling energy and hence critical current in the liquid state.[52]

To test these predictions, we have plotted $I_c(B_\perp, T)$ against $B_\perp$ on a logarithmic scale for both the argon- and oxygen-annealed samples at 25 K, just above the first peak in critical current. For both samples a power-law field dependence is observed extending over at least two orders of magnitude, with exponents $\mu=0.9$ and 0.8 for the argon- and oxygen-annealed samples, respectively, as shown in Fig. 6. This implies a high degree of misalignment of pancakes along the *c* axis, consistent with the observed major reduction in critical current with field.

CRITICAL CURRENT IN A PARALLEL MAGNETIC FIELD

For magnetic field parallel to the CuO_2 planes, the focus of most previous studies has been to look for the expected Fraunhofer-type field dependence of the *c*-axis critical current.[6,7,53] Comparatively little attention has been devoted to the Josephson vortex state and its dynamics at high fields apart from the search for thermodynamic phase transitions[54,55] and an investigation of the angular dependence of the plasma frequency $\omega_c^2 \sim J_c(B)$ with field direction.[56]

The parallel-field dependence of the *I-V* characteristics reveal several additional features, as illustrated in Fig. 7 for measurements at 25 K in a number of fields. We first note the onset of a resistive regime preceding the main critical current transition to the first resistive branch. Similar behavior has been observed in linear stacks of artificial long Josephson junctions for fields parallel to the junction, and can be identified with the flux flow resistance of Josephson vortices parallel to the junctions.[57,58] The flux flow resistivity, defined as the dynamic resistance in the resistive regime, is rather closely proportional to the magnetic field[59] (see Fig. 7).

Figure 8 compares the field dependence of the critical current $I_c(B_\parallel)$ determined from the major jump to the first

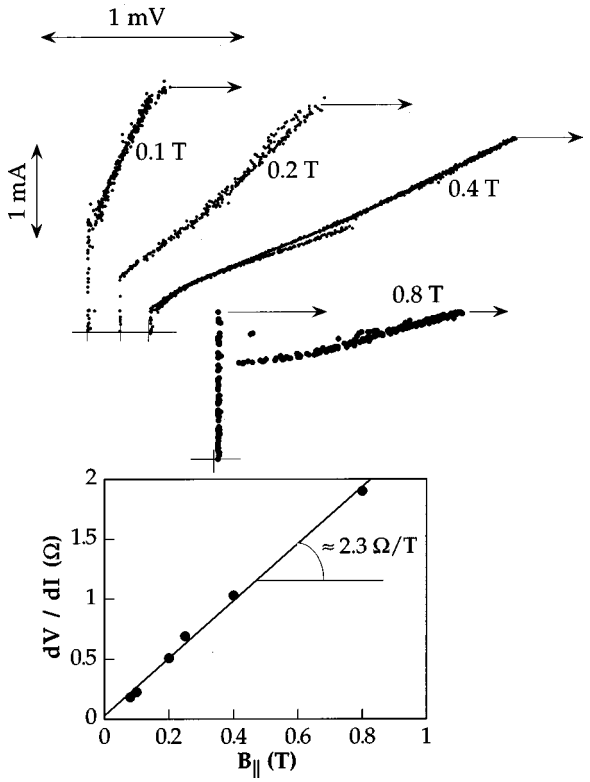

FIG. 7. *I-V* characteristics at 25 K of the argon-annealed sample as a function of $B_{\|}$ (top), and the magnetic-field-dependence of the dynamic resistance $dV/dI(B_{\|})$ for the displaced linear branch (bottom).

resistive branch (indicated by the arrows in Fig. 7) at $T=25$ K for our two samples. The critical current varies as $I_c \sim \exp(-B_{\|}/B_0)$, with $B_0 \sim 2.1$ and ~ 2.5 T for the argon- and oxygen-annealed samples, respectively. This is consistent with earlier single-crystal measurements by Latyshev and Volkov,[60] which can also be described by a nearly exponential dependence, but with a slightly larger scaling field of $B_0 \sim 3.5$ T. In contrast, theoretical models predict a power-law dependence on field, even for small misalignment between the field and *ab* plane.[46,56]

We speculate that the discrepancy between theory and experiment is due to disorder and pinning of pancakes,

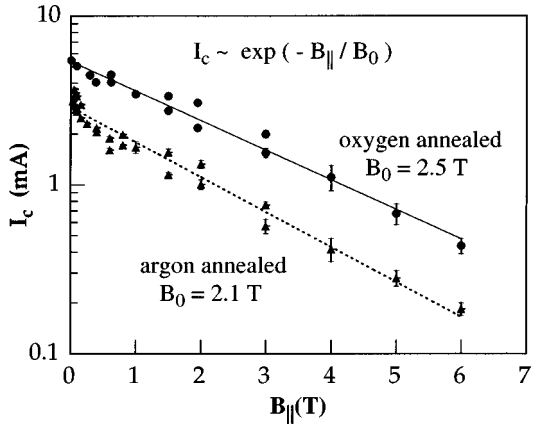

FIG. 8. $I_c(B_{\|})$ at $T=25$ K for two samples with different oxygen content.

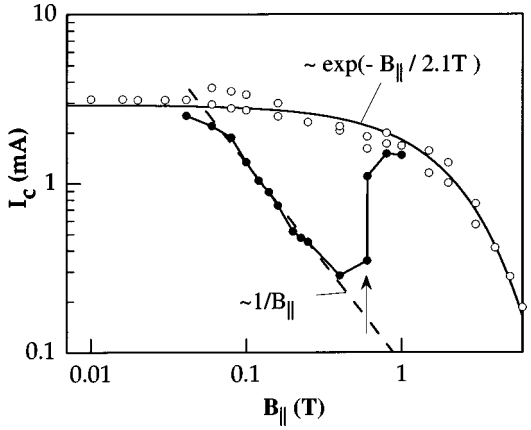

FIG. 9. $I_c(B_{\|})$ for the argon-annealed sample in low fields. Filled symbols represent the 0.1 μV threshold criterion measurements of I_c. Open symbols correspond to the major transition to the first resistive branch.

which is neglected in Ref. 56. Pancakes, resulting from flux penetration through the *ab* plane, due to a small misalignment angle θ between the magnetic field and *ab* planes, are probably strongly pinned within the planes. They are therefore unable to adjust their positions to the equilibrium Josephson vortex lattice structure as assumed in theoretical models.

Above 0.8 T we observed a qualitative change in the *c*-axis *I-V* characteristics with a sudden increase in critical current and the disappearance of the low-voltage resistive branch before the main transition. This behavior can be explained in the following way. For fields greater than 0.8 T, a small misalignment of the field may be sufficient to nucleate randomly pinned vortex pancakes within the CuO planes. such pancakes can then pin the in-plane Josephson vortices, restoring the zero-resistance state, as illustrated in Fig. 9.

The average distance between pancakes l_p is of order $(\Phi_0/B_{\|}\theta)^{1/2} \sim 500\,\text{nm} \sim \lambda_{ab}$ for $B_{\|} \sim 5$ T, (we have taken $\theta \sim 0.1°$). The distance r_J between the Josephson vortices, $(\Phi_0/B_{\|})^{1/2}$ is ~ 270 nm. The Josephson vortex lattice is expected to be rigid when the two spacings are similar and when the nonlinear parts of the Josephson vortices strongly overlap.[61] It is then necessary to invoke a collective pinning approach to calculate the critical current. Since we have assumed pancake vortices to be the main pinning centers for Josephson vortices, it is reasonable to take the characteristic Josephson vortex line pinning length L_c to be of the order of l_p or somewhat larger. When the Josephson lattice period r_J is less than L_c, the system can be considered as being in the small-bundle pinning regime. In this limit the critical current is expected to decrease exponentially with field,[19] as indeed observed.

If the Josephson vortex pinning length L_c is dictated by the pancake intervortex distance, one should be able to investigate different pinning regimes simply by adjusting the misalignment angle θ.

SUMMARY

In summary, we have measured the *c*-axis normal and superconducting transport properties across mesa stacks of intrinsic Josephson junctions in 2212-BSCCO single crystals

as a function of temperature and magnetic field perpendicular and parallel to the *ab* planes. The small size of these structures and the avoidance of high-temperature processing enable us to overcome problems from sample heating and contamination from diffusion of silver from the contact regions.

For the argon-annealed sample, we observe one of the largest *c*-axis resistance peaks yet reported, almost double that of the oxygen-annealed sample. For our crystals, we observe an inverse relationship between the peak in R_c and the critical current at zero field and temperature.

In the superconducting state, multibranched *I-V* characteristics are observed with similar critical currents and differences in voltages between each branch. The critical current is strongly depressed after cooling in a field, particularly at low temperatures. We associate this reduction with a loss of superconducting phase coherence across the CuO_2 planes resulting from the misalignment of pancake vortices within the planes, caused by weak local pinning centers, such as oxygen vacancies. On increasing temperature, there is a marked increase in critical current, consistent with the thermal activation of pancakes out of the weaker pinning centers, enabling them to improve their alignment along the *c* direction and their ordering within the planes. At a field-dependent temperature $T^*(B)$, the critical current rises to a peak and becomes more reproducible from measurement to measurement. This peak appears to coincide with a thermally activated transition above which flux pancakes in the planes can escape relatively easily from the weaker pinning centers. However, the absence of any dissipation until a considerably higher temperature $T_{\rm irr}(B_\perp)$ suggests a solid or glassy state rather than a liquid pancake fluxon state, perhaps pinned by a number of deeper pinning centers (e.g., dislocation loops or other lattice defects). At $T_{\rm irr}(B_\perp)$ the characteristics become resistive, consistent with a melting of the vortex pancake phase.

Apart from the onset of dissipation at low voltages, there is no marked change in the *I-V* characteristics at $T_{\rm irr}(B_\perp)$. A critical current can therefore still be defined, which increases slightly above $T_{\rm irr}(B_\perp)$ before decreasing to zero at $T_c(0)$. This could be explained if a number of pancakes remain strongly pinned by deep pinning centers on initially entering the liquid state. As the temperature rises they eventually become unpinned and increase their *c*-axis alignment and hence the critical current. The field and temperature dependence of the critical current in the liquid state above $T_{\rm irr}(B_\perp)$ and in the solid state at lower temperatures is in qualitative agreement with theoretical predictions, with critical current approximately inversely proportional to field.

In a parallel field, $I_c(T,B_\parallel)$ varies as $I_c=\exp(-B_\parallel/B_0)$ with B_0 in the range $\sim$2.1–2.5 T, consistent with the expected behavior of Josephson vortices in the small bundle pinning regime. At low voltages, a resistive branch is observed prior to the main resistive transition consistent with the flux flow of Josephson vortices. This branch disappeared above $\sim$0.8 T, which we identify as the field required for the slightly misaligned field to nucleate pancake vortices in the planes, which are assumed to inhibit flux flow.

ACKNOWLEDGMENTS

This research was supported by the Swedish Superconductivity Consortium and the Swedish Royal Academy of Sciences through its Nobel Institute. Photolithography was performed in the Swedish Nanometer Laboratory. The measurements in a magnetic field were conducted in Birmingham within the interdisciplinary Superconductivity program supported by the EPSRC, who also support the National Crystal Growth Facility for Superconducting Oxides providing the crystals. The expert technical support provided by G. Walsh and P. Andrews is greatly appreciated. A. Yurgens is grateful for support and hospitality during experiments undertaken in Birmingham.

*On leave from P. L. Kapitza Institute, Moscow, Russia; electronic address: yurgens@fy.chalmers.se

[1] L. L. Daemen, L. N. Bulaevskii, M. P. Maley, and J. Y. Coulter, Phys. Rev. Lett. **70**, 1167 (1993).

[2] L. Daemen, L. N. Bulaevskii, M. P. Maley, and J. Y. Coulter, Phys. Rev. B **47**, 11 291 (1993).

[3] A. E. Koshelev, L. I. Glasman, and A. I. Larkin, Phys. Rev. B **53**, 2786 (1996).

[4] G. Blatter, V. Geshkenbein, A. Larkin, and H. Nordborg, Phys. Rev. B **54**, 72 (1996).

[5] W. Lawrence and S. Doniach, in *Proceedings of the Twelfth International Conference on Low Temperature Physics*, Kyoto, Japan, edited by E. Kanda (Keigaku, Tokyo, 1971), p. 361.

[6] R. Kleiner, F. Steinmeyer, G. Kunkel, and P. Müller, Phys. Rev. Lett. **68**, 2394 (1992).

[7] R. Kleiner and P. Müller, Phys. Rev. B **49**, 1327 (1994).

[8] S. Luo, G. Yang, and C. E. Gough, Phys. Rev. B **51**, 6655 (1995).

[9] J. H. Cho, M. P. Maley, S. Fleshler, A. Lacerda, and L. N. Bulaevskii, Phys. Rev. B **50**, 6493 (1994).

[10] A. Yurgens, D. Winkler, N. V. Zavaritsky, and T. Claeson, Appl. Phys. Lett. **70**, 1760 (1997).

[11] R. Cubitt, E. M. Forgan, G. Yang, S. L. Lee, D. M. Paul, H. A. Mook, M. Yethiraj, P. H. Kes, T. W. Li, A. A. Menovsky, Z. Tarnawski, and K. Mortensen, Nature (London) **365**, 407 (1993).

[12] S. L. Lee, P. Zimmerman, H. Keller, M. Warden, I. M. Savić, R. Schauwecker, D. Zech, R. Cubitt, E. M. Forgan, P. H. Kes, T. W. Li, A. A. Menovsky, and Z. Tarnawski, Phys. Rev. Lett. **71**, 3862 (1993).

[13] B. Khaykovich, M. Konczykowski, E. Zeldov, R. A. Doyle, D. Majer, P. H. Kes, and T. W. Li, Phys. Rev. B **56**, R517 (1997).

[14] E. Zeldov, D. Majer, M. Konczykowski, V. B. Geshkenbein, V. M. Vinokur, and H. Shtrikman, Nature (London) **375**, 373 (1995).

[15] H. Safar, P. L. Gammel, D. J. Bishop, D. B. Mitzi, and A. Kapitulnik, Phys. Rev. Lett. **68**, 2672 (1992).

[16] H. Safar, P. L. Gammel, D. A. Huse, D. J. Bishop, W. C. Lee, J. Giapintzakis, and D. M. Ginsberg, Phys. Rev. Lett. **70**, 3800 (1993).

[17] O. K. C. Tsui, N. P. Ong, Y. Matsuda, Y. F. Yan, and J. B. Peterson, Phys. Rev. Lett. **73**, 724 (1994).

[18] Y. Matsuda, M. B. Gaifullin, K. Kumagai, K. Kadowaki, and T. Mochiki, Phys. Rev. Lett. **75**, 4512 (1995).

[19] G. Blatter, M. V. Feigel'man, V. B. Geshkenbein, A. I. Larkin, and V. M. Vinokur, Rev. Mod. Phys. **66**, 1125 (1994).

[20] G. Yang, C. E. Gough, and J. S. Abell, IEEE Trans. Appl. Supercond. **3**, 1663 (1993).

[21] G. Yang, P. Shang, S. D. Sutton, I. P. Jones, J. S. Abell, and C. E. Gough, Phys. Rev. B **48**, 4054 (1993).
[22] A. K. Pradhan, S. B. Roy, P. Chaddah, C. Chen, and B. M. Wanklyn, Phys. Rev. B **49**, 12 984 (1994).
[23] F. Zuo, S. Khizroev, G. C. Alexandrakis, and V. N. Kopoylov, Phys. Rev. B **52**, R755 (1995).
[24] R. Busch, G. Ries, H. Werthner, G. Kreiselmeyer, and G. Saemann-Ischenko, Phys. Rev. Lett. **69**, 522 (1992).
[25] In a few cases, a 60-fold increase of $R_c(T,5\ \mathrm{T})$ / $R_c(150\ \mathrm{K})$ was observed, see D. Winkler, A. Yurgens, and T. Claeson (unpublished).
[26] G. Briceno, M. F. Crommie, and A. Zettl, Phys. Rev. Lett. **66**, 2164 (1991).
[27] M. C. Hellerqvist, S. Ryu, L. W. Lombardo, and A. Kapitulnik, Physica C **230**, 170 (1994).
[28] Y. F. Yan, P. Matl, J. M. Harris, and N. P. Ong, Phys. Rev. B **52**, R751 (1995).
[29] A. S. Alexandrov, V. N. Zavaritsky, W. Y. Liang, and P. L. Nevsky, Phys. Rev. Lett. **76**, 983 (1996).
[30] A. Yurgens, D. Winkler, N. V. Zavaritsky, and T. Claeson, Phys. Rev. Lett. **79**, 5122 (1997).
[31] S. L. Cooper and K. E. Gray, in *Physical Properties of High Temperature Superconductors IV*, edited by D. M. Ginsburg (World Scientific, Singapore, 1994), Vol. 4, p. 61.
[32] L. Ioffe, A. I. Larkin, A. A. Varlamov, and L. Yu, Phys. Rev. B **47**, 8936 (1993).
[33] V. V. Dorin, R. A. Klemm, A. A. Varlamov, A. I. Buzdin, and D. V. Livanov, Phys. Rev. B **48**, 12 951 (1993).
[34] K. E. Gray and D. H. Kim, Phys. Rev. Lett. **70**, 1693 (1993).
[35] A. S. Nygmatulin, A. A. Varlamov, D. V. Livanov, G. Balestrino, and E. Milani, Phys. Rev. B **53**, 3557 (1996).
[36] T. Hasegawa, H. Ikuta, and K. Kitazawa, in *Physical Properties of High Temperature Superconductors III*, edited by D. M. Ginsberg (World Scientific, Singapore, 1992), Vol. 3, p. 525.
[37] C. Renner and Ø. Fisher, Phys. Rev. B **51**, 9208 (1995).
[38] A. Yurgens, D. Winkler, N. V. Zavaritsky, and T. Claeson, Phys. Rev. B **53**, R8887 (1996).
[39] T. A. Fulton and L. N. Dunkleberger, Phys. Rev. B **9**, 4760 (1974).
[40] V. M. Krasnov and D. Winkler, Phys. Rev. B **56**, 9106 (1997).
[41] V. Ambegaokar and B. J. Halperin, Phys. Rev. Lett. **22**, 1364 (1969).
[42] M. F. Goffman, J. A. Herbsommer, F. d. l. Cruz, T. W. Li, and P. H. Kes, Phys. Rev. B **57**, 3663 (1998).
[43] D. T. Fuchs, E. Zeldov, D. Majer, R. A. Doyle, T. Tamegai, S. Ooi, and M. Konczykowski, Phys. Rev. B **54**, R796 (1996).
[44] S. H. Lloyd, C. M. Aegerter, S. L. Lee, E. M. Forgan, C. Ager, S. Romer, R. Cubitt, S. T. Johnson, D. M. Paul, H. Keller, M. Y. Wylie, and M. P. Nutley (unpublished).
[45] D. Ertas and D. R. Nelson, Physica C **272**, 79 (1996).
[46] L. N. Bulaevskii, V. L. Pokrovsky, and M. P. Maley, Phys. Rev. Lett. **76**, 1719 (1996).
[47] V. N. Zavaritsky and N. V. Zavaritsky, Pis'ma Zh. Eksp. Teor. Fiz. **54**, 25 (1991) [JETP Lett. **54**, 23 (1991)]; **54**, 335 (1991) [**54**, 330 (1991)].
[48] K. Krishana, N. P. Ong, Q. Li, G. D. Gu, and N. Koshizuka, Science **277**, 83 (1997).
[49] L. I. Glazman and A. E. Koshelev, Phys. Rev. B **43**, 2835 (1991).
[50] D. R. Nelson and B. I. Halperin, Phys. Rev. B **19**, 2457 (1979).
[51] A. E. Koshelev, Phys. Rev. Lett. **76**, 1340 (1996).
[52] A. E. Koshelev, Phys. Rev. Lett. **77**, 3901 (1996).
[53] Y. I. Latyshev, J. E. Nevelskaya, and P. Monceau, Phys. Rev. Lett. **77**, 932 (1996).
[54] V. N. Zavaritsky, Phys. Scr. **T66**, 230 (1996).
[55] M. S. Fuhrer, K. Ino, K. Oka, Y. Nishihara, and A. Zettl, Solid State Commun. **101**, 841 (1997).
[56] L. N. Bulaevskii, M. Maley, H. Safar, and D. Domínguez, Phys. Rev. B **53**, 6634 (1996).
[57] A. C. Scott and W. E. Johnson, Appl. Phys. Lett. **14**, 316 (1969).
[58] N. F. Pedersen, in *Solitons*, edited by S. E. Trullinger, V. E. Zakharov, and V. L. Pokrovsky (Elsevier, Amsterdam, 1986), p. 469.
[59] J. U. Lee and J. E. Nordman, Physica C **277**, 7 (1997).
[60] Y. I. Latyshev and A. F. Volkov, Physica C **182**, 47 (1991).
[61] L. N. Bulaevskii, D. Domíngues, M. P. Maley, A. R. Bishop, and B. I. Ivlev, Phys. Rev. B **53**, 14 601 (1996).
[62] C. D. Keener, M. L. Trawick, S. M. Ammirata, S. E. Hebboul, and J. C. Garland, Phys. Rev. Lett. **78**, 1118 (1997).